Sensitivity Analysis Of An In Silico Model Of Tumor Growth And Radiation Response

C. Sosa Marrero, Oscar Acosta, M. Castro, A. Hernandez, N. Rioux-Leclercq, F. Paris, R. de Crevoisier

2019 IEEE 16th International Symposium on Biomedical Imaging (ISBI 2019)
Venice, Italy, April 8-11, 2019

SENSITIVITY ANALYSIS OF AN *IN SILICO* MODEL OF TUMOR GROWTH AND RADIATION RESPONSE

C. Sosa Marrero[1]*, O. Acosta*[1]*, M. Castro*[1]*, A. Hernández*[1]*, N. Rioux-Leclercq*[1]*, F. Paris*[2] *and R. de Crevoisier*[1]

[1]Univ Rennes, CHU Rennes, CLCC Eugène Marquis, INSERM, LTSI - UMR 1099, F-35000 Rennes, France
[2]CRCINA, INSERM, CNRS, Université de Nantes, Nantes, France.

ABSTRACT

Simulating the response to radiotherapy (RT) in cancer patients may help devising new therapeutic strategies. Computational models make it possible to cope with the multi-scale biological mechanisms characterising this group of diseases. We present in this paper an *in silico* model of tumour growth and radiation response, capable of simulating a whole RT protocol of prostate cancer. Oxygen diffusion, proliferation of tumour cells, angiogenesis based on the VEGF diffusion, oxygen-dependent response to irradiation and resorption of dead cells were implemented in a multi-scale framework. A sensitivity analysis using the Morris screening method was performed on 21 computational tissues, initialised from prostate histopathological specimens presenting different tumour and vascular densities. The dose per fraction and the duration of the cycle of tumour cells were identified as the most important parameters of the model.

Index Terms— Computational modelling, tumour growth, radiotherapy, prostate cancer, sensitivity analysis

1. INTRODUCTION

Cancer is currently the main cause of mortality in many developed countries. Prostate cancer, specifically, is the most often diagnosed type of cancer in men from 82 countries with high and very high human development indexes [1]. Among the numerous existing treatments, external RT is the most commonly used. It is estimated that 52.3% of all cancer patients receive RT at some point during their treatment [2]. This percentage rises up to 60% for prostate cancer patients. To allow healthy tissues enough time to recover, the radiation process is carried out over several sessions. In prostate RT, a total dose of 80 Gy with a scheme of 2 Gy/fraction during eight weeks from Monday to Friday is typically prescribed, achieving, in most of the cases, tumour local control at the end of the treatment.

However, about 0-10%, 10-20% and 30%-40% of patients with, respectively low, intermediate and high risk tumours (according to the D'Amico classification) suffer a relapse within 5 years [3]. To improve these numbers, hypofractionated treatments have been recently proposed [4]. They suggest increasing the dose per fraction d, reducing the number of irradiation sessions N. The knowledge of the response of patients to these new schemes is still limited.

Computational models appear as attractive tools to deal with this issue. They have been used for simulating and quantitatively analysing several human physiological processes with the aim of using the results for diagnosis and improved therapeutic applications [5]. The principles of computational modelling and the difficulties arising when integrating mechanisms occurring at different temporal and spatial scales and described by various formalisms are thoroughly discussed by Hernández et al. [6].

Another major issue of *in silico* models is to deal with the large number of variables they may contain. Sensitivity analysis are helpful to identify the most relevant parameters, determine which ones can be negligible and potentially simplify the model. Sobol variance-based method [7] is capable of determining quantitatively the impact of parameters on a given output of the model. However, it is computationally expensive. Morris screening method [8] offers a rough view of the hierarchy of parameters of a model with a limited cost.

We propose in this paper a multi-scale computational model going further from Aubert et al. [9] and integrating (i) oxygenation of the tissue, (ii) proliferation of tumour cells, (iii) angiogenesis, (iv) oxygen-dependent response to irradiation and (v) resorption of dead cells. The model was implemented in C++, using the Multi-formalism Modeling and Simulation Library (M2SL) [5] [10], previously developed in our laboratory. To identify the most relevant parameters of the model, as well as to characterise the nature of their impact on a given output, a sensitivity analysis using the Morris screening method was performed.

The paper is structured as follows: next section describes the tumour growth and response to RT model as well as the principles of the Morris screening method. Then, the results of this analysis are presented.

2. MATERIALS AND METHODS

2.1. Description of the tumour growth and response to RT model

2.1.1. General description

We considered a 3D prostate computational tissue, containing 7 types of cells: healthy (fibroblasts, macrophages, epithelial, smooth muscle, etc) tumour, pre-existing and neo-created endothelial and dead by hypoxic necrosis, apoptosis or mitotic catastrophe. Each voxel of the tissue corresponds to one cell of the above-mentioned types. Tissues were initialised using hispathological specimens from patients with localised prostate cancer treated with radical prostatectomy (figure 1).

2.1.2. Oxygenation

Oxygenation of the tissue was modelled using the reaction-diffusion equation (1) [11] with the partial oxygen pressure $pO_2(x,t)$ as unknown; D^{O_2}, the diffusion coefficient; $V_{max}^{O_2}$, the maximum oxygen

consumption ratio and $K_M^{O_2}$, the Michaelis constant.

$$\frac{\partial pO_2}{\partial t} = D^{O_2}\Delta pO_2 - V_{max}^{O_2}\frac{pO_2}{pO_2 + K_M^{O_2}}, \quad (1)$$

We considered that dead cells do not consume oxygen. We supposed that pre-existing and neo-created endothelial cells have fixed pO_2 values pO_2^{preEnd} and pO_2^{neoEnd}, respectively. We considered that cells having a pO_2 lower than a threshold pO_2^{nec} die instantaneously by hypoxic necrosis.

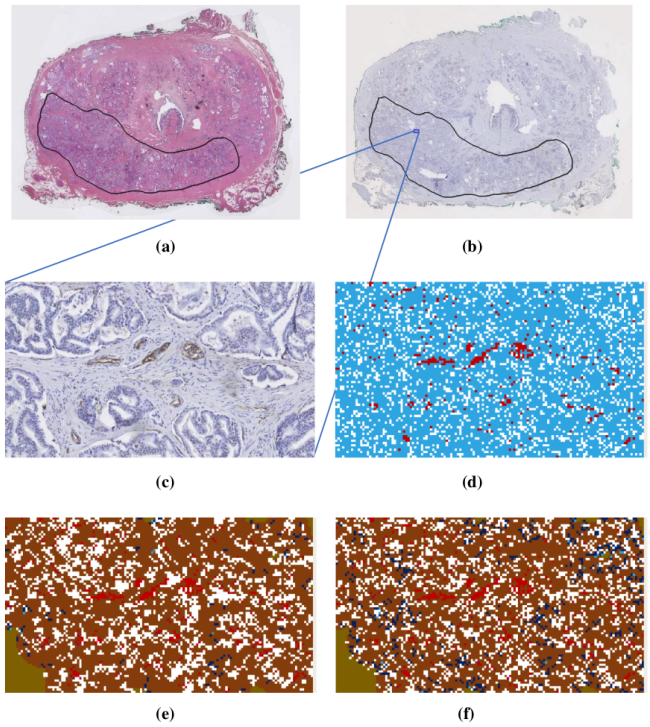

Fig. 1. Example of an (a) HES staining of an histopathological cut; (b) corresponding CD31 staining; (c) CD31 staining region of interest; (d) initial computational tissue, where healthy cells are represented in white; tumour, in light blue and pre-existing endothelial in light red; (e) computational tissue after a 37 × 2 Gy RT treatment [12], where tumour cells with DNA damaged by irradiation are represented in dark blue; neo-created endothelial, in dark red and dead by hypoxic necrosis, in ochre and by mitotic catastrophe, in brown and (f) computational tissue after a 20 × 3 RT treatment [12].

2.1.3. *Proliferation of tumour cells*

To reproduce the proliferation of tumour cells, the life-cycle represented in figure 2 was considered. It is composed of four phases: G1, S, G2 and M. There exists a fifth phase, called G0 and placed out of the cycle, in which cells are quiescent. When a cell whose DNA has not been damaged by irradiation, arrives at the end of its cycle, it divides, placing the new tumour cell in an available space (a healthy or dead cell) of its Moore neighbourhood of order N. If there is no free place around, then the cell enters the G0 phase, where it remains until the liberation of a space. The duration of each phase can be calculated using the percentages of figure 2.

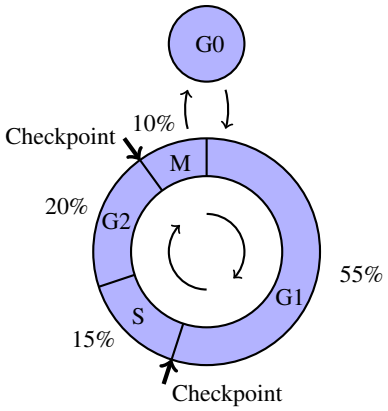

Fig. 2. Cell cycle

2.1.4. *Angiogenesis*

The modelling of angiogenesis, was based on the VEGF (Vascular endothelial growth factor) diffusion. This protein, consumed by endothelial cells, is emitted by hypoxic cells to provoke the creation of blood vessels that satisfy their oxygen needs. We considered that the VEGF distribution $v(x,t)$ is given by the reaction-diffusion equation (2)

$$\frac{\partial v}{\partial t} = D^{VEGF}\Delta v - V_{max}^{VEGF}\frac{v}{v + K_M^{VEGF}}, \quad (2)$$

where D^{VEGF} is the diffusion coefficient; V_{max}^{VEGF}, the maximum VEGF consumption ratio and K_M^{VEGF}, the Michaelis constant. We supposed that hypoxic cells (with a pO_2 value lower than a given threshold pO_2^{hyp}) have a fixed $v(x,t)$ value, v^{hyp}. Different cycle durations T_{preEnd} and T_{neoEnd}, were defined for pre-existing and neo-created endothelial cells, respectively. If at the end of the cycle, the VEGF concentration of an endothelial cell whose DNA has not been damaged by irradiation exceeds a predetermined value $\bar{v}$, the cell in question divides. If not, it enters the quiescent phase G0, where it remains until a potential augmentation of $v(x,t)$. The new endothelial cell is placed in the most hypoxic direction.

2.1.5. *Response to irradiation*

To model the response of every cell to irradiation, its survival fraction (SF) was calculated using the linear-quadratic equation, as it is done in almost every other model in the literature, adjusted to consider the influence of the pO_2 (3) [13].

$$SF = \exp\left(-\frac{\alpha}{m}d\,OER - \frac{\beta}{m^2}d^2 OER^2\right), \quad (3)$$

where α and β are the radiosensitivity parameters; d, the administered dose per session and OER, the oxygen enhancement ratio. We considered that the radiosensitivity of tumour cells varies throughout the cycle. The other types of cells, significantly more radioresistant, have constant values of α and β throughout the cycle. Irradiated cells are arrested for a duration T_{arrest} at checkpoints situated in transitions between phases G1/S and G2/M [14] (figure 2). For low doses ($d \leq d^{thres}$), cells damaged by irradiation die by mitotic catastrophe. For high doses ($d > d^{thres}$), they do it instantaneously by apoptosis.

Table 1. Ranges of factors

Factor	Range
T_{tum}	85,68 - 1310,4 h [13][15]
T_{heal}	171,36 - 2620,8 h
T_{neoEnd}	1680 - 3120 h
$\bar{v}$	10,5 mol/μm^3 - 19,5 mol/μm^3
α_{heal}	$7 \cdot 10^{-4}$ - $1,3 \cdot 10^{-3}$ Gy^{-1}
α/β_{heal}	0,7 - 13 Gy
α_{tumG1}	0,0238 - 0,3562 Gy^{-1} [4]
α/β_{tumG1}	0,7 - 13 Gy [4]
α_{tumS}	0,0168 - 0,2561 Gy^{-1} [4]
α/β_{tumS}	0,7 - 13 Gy [4]
α_{tumG2}	0,0252 - 0,3809 Gy^{-1} [4]
α/β_{G2}	0,7 - 13 Gy [4]
α_{tumM}	0,028 - 0,4251 Gy^{-1} [4]
α/β_{tumM}	0,7 - 13 Gy [4]
α_{tumG0}	0,105 - 0,195 Gy^{-1}
α/β_{tumG0}	0,7 - 13 Gy
α_{preEnd}	$7 \cdot 10^{-4}$ - $1,3 \cdot 10^{-3}$ Gy^{-1} [14]
α/β_{preEnd}	0,7 - 13 Gy [14]
α_{neoEnd}	$7 \cdot 10^{-4}$ - $1,3 \cdot 10^{-3}$ Gy^{-1} [14]
α/β_{neoEnd}	0,7 - 13 Gy [14]
d_{thres}	4,2 - 13 Gy
T_{arrest}	4,2 - 39 h
pO_2^{nec}	0,7 - 1,3 mmHg [14]
d	1,26 - 6,5 Gy
D^{O_2}	1,022 - 2,873 μm^2/ms [11]
$V_{max}^{O_2}$	5,81 $\cdot 10^{-3}$ - 2,873 $\cdot 10^{-2}$ mmHg/ms [11]
$K_M^{O_2}$	0,119 - 7,67 mmHg [11]
D^{VEGF}	1,4 - 2,6 μm^2/ms
V_{max}^{VEGF}	5,25 $\cdot 10^{-3}$ - 6,825 $\cdot 10^{-3}$ mol/μm^{3}ms
K_M^{VEGF}	1,75 - 3,25 mol/μm^3
pO_2^{preEnd}	8,4 - 93,6 mmHg [16]
pO_2^{neoEnd}	8,4 - 93,6 mmHg [16]
pO_2^{hyp}	3,5 - 6,5 mmHg [14]
v^{hyp}	14 - 26 mol/μm^3

2.1.6. Resorption of dead cells

We considered the resorption of dead cells as the result of a competition between the proliferation of tumour cells described in subsection 2.1.3 and the division of healthy cells, for which the duration of their cycle T_{heal} is defined. When a cell whose DNA has not been damaged by irradiation, arrives at the end of its cycle, it divides, replacing a dead cell of its Moore neighbourhood of order N by a new healthy cell. If there is no dead cell around, then it enters the G0 phase.

2.2. Description of the Morris screening method

This method explores a K-dimensional cube, where K is the number of factors, regularly divided in p levels. In this space, N elementary effects, given by (4)

$$EE_i = \frac{f(x_1, ..., x_i, ..., x_K) - f(x_1, ..., x_i + \Delta, ..., x_K)}{\Delta}, \quad (4)$$

are calculated for each factor x_i. Morris suggests using a clever experimental plan that requires, in total, $N(K+1)$ simulations of the model and taking $\Delta = \frac{p}{2(p-1)}$, where p is even. Thus, the mean and standard values ($\mu_i \pm \sigma_i$) are computed for each parameter. To avoid the cancellation of symmetrical elementary effects, more recent works (Campolongo et al. [17]) propose considering the mean over the absolute value of elementary effects, μ_i^*. Studying in the plane μ^* vs. σ the obtained mean and standard deviation values, we can distinguish three regions: factors with low μ_i^* and σ_i can be considered negligible, those with high μ_i^* and low σ_i have a linear effect on the model output and those with high μ_i^* and σ_i possess either a non-linear effect on the output model or an important interaction with other factors.

The time to destroy 95% of initial tumour cells was used as output of the model. We considered the ranges presented in table 1 for the $K = 34$ parameters of the model. They were obtained calculating, respectively, 0.7 and 1.3 of the minimum P^{min} and maximum P^{max} values extracted from the literature. The value of Δ used for each parameter was normalised as $\frac{\Delta}{1.3P^{max} - 0.7P^{min}}$.

3. RESULTS AND DISCUSSION

We present the results of the Morris sensitivity analysis performed on the 21 computational tissues, taking $p = 20$ and $N = 100$. We considered for every simulation a total dose of 80 Gy, administered every 24 h, from Monday to Friday.

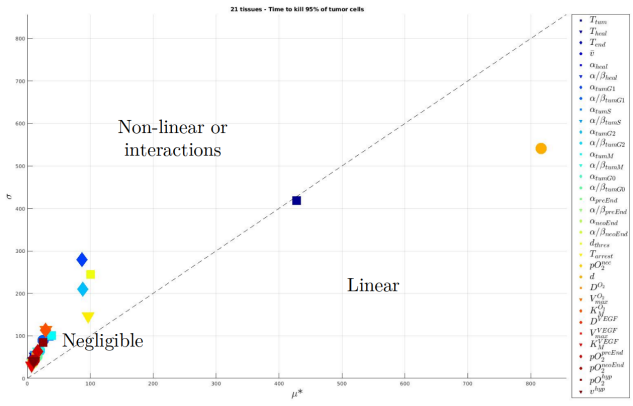

Fig. 3. Mean $\mu*$ vs. σ plane for the 21 computational tissues

We represent in figure 3 the means and standard deviations of the elementary effects of the 34 parameters of the model. We observe that the dose per fraction d is situated in the linear region. The duration of the cycle of tumour cells is situated on the axis $\sigma = \mu*$. In the "non-linear or interactions" region, we can find α_{tumG1}, d_{thres}, α_{tumG2} and T_{arrest}. The rest of the parameters could be considered negligible. The σ components of d and d_{thres} may be explained by the existing interaction between them. In fact, as described in

subsection 2.1.5, $d < d^{thres}$ results in immediate death of irradiated cells and, consequently, significantly lower values of time to kill 95% of initial tumour cells.

In figure 4, we present the mean Euclidean distance to the origin of points in figure 3 and the respective $\mu*$ contribution, calculated as $\frac{\mu*^2}{\sqrt{\mu*^2+\sigma^2}}$. We observe that the dose per fraction d has the highest impact on the output of the model. The duration of the cycle of tumour cells T_{tum} presents the second most important effect.

The response of tissues to different doses per fraction, in particular to high values corresponding to hypofractionated treatments, will be discussed in depth in future works. As a first step, we have tested two irradiation schemes of 37 $\times$ 2 Gy (figure 1.e) and 20 $\times$ 3 Gy (figure 1.f) every 24h from Monday to Friday, whose equivalence in terms of relapse within 5 years has been pointed out in clinical studies [12].

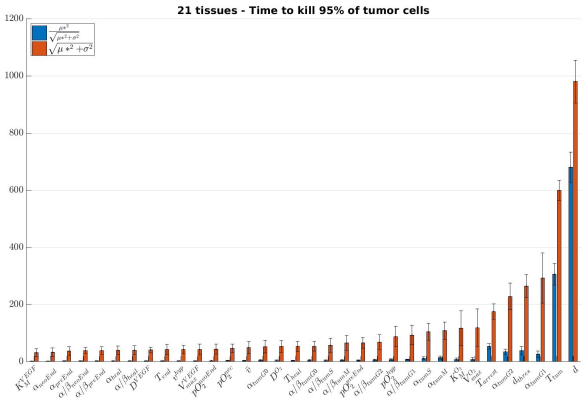

Fig. 4. Mean Euclidean distance to the origin (in red) and its $\mu*$ contribution (in blue) for the 21 computational tissues

4. CONCLUSION

We developed a multi-scale *in silico* model of tumor growth and oxygen-dependent response to radiation. The Morris analysis performed on the 21 computational tissues determined that the dose per fraction and the duration of the cycle of tumour cells have the most important effect on the time needed to kill 95% of initial tumour cells. A global sensitivity analysis using the Sobol method will be performed to better evaluate the impact of these parameters. In particular, understanding the effect of the dose per fraction is essential to predict the patients response to different hypofractionated treatments before applying them in clinics.

5. REFERENCES

[1] F. Bray, A. Jemal, N. Grey, J. Ferlay, and D. Forman, "Global cancer transitions according to the human development index (2008-2030): A population-based study," *Lancet Oncol.*, vol. 13(8), pp. 790–801, 2012.

[2] M. Joiner and A. van der Kogel, *Basic Clinical Radiobiology*, Hodder Arnold, London, 2009.

[3] K. Gnep, A. Fargeas, R. E. Gutierrez-Carvajal, F. Commandeur, R. Mathieu, and J. D. Ospina. et al., "Haralick textural features on t2-weighted mri are associated with biochemical recurrence following radiotherapy for peripheral zone prostate cancer," *J Magn Reson Imaging*, vol. 45, pp. 103–117, 2017.

[4] D. J. Brenner and E. J. Hall, "Hypofractionation in prostate cancer radiotherapy," *Translational Cancer Research*, vol. 7, no. 6, 2018.

[5] A. I. Hernandez, V. Le Rolle, A. Defontaine, and G. Carrault, "A multiformalism and multiresolution modelling environment: application to the cardiovascular system and its regulation," *Philos Transact. A Math. Phys. Eng. Sci.*, vol. 367(1908), pp. 4923–4940, 2009.

[6] A. I Hernndez., V. Le Rolle, D. Ojeda, P. Baconnier, J. Fontecave-Jallon, F. Guillaud, and T. Grosse et al., "Integration of detailed modules in a core model of body fluid homeostasis and blood pressure regulation," *Progress in Biophysics and Molecular Biology*, vol. 107, no. 1, pp. 169–182, 2011.

[7] I. M. Sobol', "Sensitivity estmiates for non linear mathematical models," *Mathematical Modelling and Computational Experiments*, vol. 1, pp. 407–414, 1993.

[8] M. Morris, "Factorial sampling plans for preliminar computational experiments," *Technometrics*, vol. 33.2, pp. 161–174, 1991.

[9] V. Aubert, O. Acosta, N. Rioux-Leclercq, R. Mathieu, F. Commandeur, and R. de Crevoisier, "In silico model to simulate the radiation response at various fractionation from histopathological images of prostate tumors," in *ISBI 2017*, pp. 818–821.

[10] D. Ojeda, V. Le Rolle, H. M. Romero-Ugalde, C. Gallet, J-L. Bonnet, and C. Henry et al., "Sensitivity analysis of vagus nerve stimulation parameters on acute cardiac autonomic responses: Chronotropic, inotropic and dromotropic effects," *PLoS ONE 11(9): e0163734*, 2016.

[11] I. Espinoza, P. Peschke, and C. P. Karger, "A model to simulate the oxygen distribution in hypoxic tumors for different vascular architectures," *Medical Physics*, vol. 40, 2013.

[12] A. Wilkins, H. Mossop, and I. Syndikus et al., "Hypofractionated radiotherapy versus conventionally fractionated radiotherapy for patients with intermediate-risk localised prostate cancer: 2-year patient-reported outcomes of the randomised, non-inferiority, phase 3 chhip trial," *Lancet Oncol*, vol. 16, pp. 1605–1616, 2015.

[13] I. Espinoza, P. Peschke, and C. P. Karger, "A voxel-based multiscale model to simulate the radiation response of hypoxic tumor," *Medical Physics*, vol. 42.1, pp. 90–102, 2015.

[14] P. Paul-Gilloteaux, V. Potiron, G. Delpon, S. Supiot, S. Chiavassa, F. Paris, and S. V. Costes, "Optimizing radiotherapy protocols using computer automata to model tumour cell death as a function of oxygen diffusion processes," *Scientific Reports*, vol. 7, 2017.

[15] A. Haworth, S. Williams, H. Reynolds, D. Waterhouse, G. M. Duchesne, J. Bucci, and M. Elbert, "Validation of a radiobiological model for low-dose-rate prostate boost focal therapy treatment planning," *Brachytherapy*, vol. 12(6), pp. 628–636, 2013.

[16] M. W. Dewhirst, E. T. Ong, B. Klitzman, T. W. Secomb, R. Z. Vinuya, R. Dodge, D. Brizel, and J. F. Gross, "Perivascular oxygen tensions in a transplantable mammary tumor growing in a dorsal flap window chamber," *Radiation Research*, vol. 130, no. 2, pp. 171–182, 1992.

[17] F. Campolongo, J. Cariboni, A. Saltelli, and W. Schoutens, "Enhancing the Morris method," *Proceedings of SAMO 2004*.